Monte-Carlo simulation of electron properties in rf parallel plate capacitively coupled discharges

M. J. Kushner [a)]
Lawrence Livermore National Laboratory, University of California, Livermore, California 94550

(Received 11 March 1983; accepted for publication 11 May 1983)

Electron properties in a parallel plate capacitively coupled rf discharge are studied with results from a Monte-Carlo simulation. Time averaged, spatially dependent electron distributions are computed by integrating, in time, electron trajectories as a function of position while oscillating the applied electric field at rf frequencies. The dc component of the sheath potential is solved for in a self-consistent manner during the simulation. For conditions where the secondary emission coefficient for electrons from the electrodes is large, the electron distribution is spatially differentiated, being dominated by an *e*-beam component near the electrodes while being nearly in equilibrium with the applied electric field in the body of the plasma. The dc component of the sheath potential is found to be a function of the ratio λ/d, where λ is the electron mean free path and d is the electrode spacing.

PACS numbers: 52.80.Pi, 52.25.Fi, 52.65. + z, 51.50. + v

I. INTRODUCTION

During the last few years there has been a resurgence of interest in low pressure, radio frequency (rf) discharges as a result of their use for plasma processing in the semiconductor industry.[1–6] In one application, plasma etching, a low pressure (<100 mTorr) rf discharge is sustained in halogenated gases. Neutral radicals and charged species diffuse or drift out of the plasma under the influence of electric fields, and are adsorbed on masked semiconductor wafers. After reacting on the surface with the lattice atoms, the products desorb as a volatile gas thereby etching the surface. An example of this process is the rapid etching of silicon in CF_4/O_2 plasmas.[7]

A typical plasma etching reactor consists of circular planar electrodes tens of centimeters in diameter and separated by a few to 10 centimeters. One or more of the electrode surfaces are covered by a dielectric surface (perhaps the wafers themselves) or a capacitor is in series with the electrodes and power supply, usually as part of an impedance matching network. This geometry is called capacitively coupled. The rf frequency is usually a few to tens of megahertz, with 13.56 MHz being an industry standard. The peak-to-peak applied potential is many hundreds of volts.

Consider the conditions for which the random electron current in the plasma is large compared to both the random ion current (positive and negative) and the rms displacement current required to charge the series capacitance of the network to the peak rf voltage. Under these conditions, the electrodes surfaces can develop a large negative bias with respect to the plasma potential.[4,8–10] The sheath potential at the surface of the electrodes has an rf and a dc component. If the electrodes have equal areas, the rf component is equal in magnitude but opposite in sign from that of the opposing electrode. The dc component is usually greater (negative) than one-quarter the peak-to-peak rf voltage thereby insuring that the net sheath potential is negative.

The dc component of the sheath potential develops as a consequence of the large disparity in mobility between electrons and ions, and the requirement that in the steady state the net current to either electrode sum to zero during an rf cycle. For rf frequencies of many megahertz, ions are accelerated to only a small fraction of their thermal velocity in the direction of the applied electric field during any half cycle. Therefore, to first order, the ion current entering the sheath is equal to the sum of the ion diffusion flux and the product of the ion density times the velocity at which the rf sheath expands into the plasma. This flux must in turn equal the total ionization rate. The electrons, though, are highly mobile and as a result, the electron current collected during the half cycle when $V_{rf}>0$ can be much greater than the current collected during the half cycle when $V_{rf}<0$. Consequently, during the first few rf cycles of the discharge the electrodes collect an excess of electron current, and a negative dc bias begins to develop. The dc bias continues to increase until the sum of the dc and rf sheath voltages are on the average sufficiently negative that the electron and ion current collected during any one rf cycle are equal. This process is analogous to the method that floating surfaces immersed in a plasma become negatively charged.[11]

For conditions where the rms displacement current through the plasma is comparable to the random electron current, the rf sheath potentials will be asymetric thereby providing the electromotive force to generate the required charging current. This situation can also occur if the electrodes have unequal areas.[9] If there is a significant density of negative ions, the dc bias decreases proportionally to the ratio of the random negative ion current to the random electron current. In the limit that the negative ion flux is much larger than the electron flux $[N_I(T_I/M_I)^{1/2} \gg n_e(T_e/m_e)^{1/2}]$ there is no dc bias. For these conditions, the sheath potential at each electrode is approximately equal to half the instantaneous rf potential, oscillating with a mean value equal to the plasma potential.

[a)] Work performed under the auspices of the U.S. Department of Energy at Lawrence Livermore National Laboratory under Contract No. W-7405-Eng-48. Present address: Mathematical Sciences Northwest, 2755 Northrup Way, Bellevue, WA 98004

 © 1983 American Institute of Physics

Downloaded 27 Mar 2003 to 128.174.115.149. Redistribution subject to AIP license or copyright, see http://ojps.aip.org/japo/japcr.jsp

There are two distinct regions with respect to the flow of electron energy in a parallel plate rf discharge: the bulk plasma and the sheaths. In the bulk plasma, energy is coupled into the electrons at a rate proportional to the applied electric field, subject to certain constraints. Consider the conditions where $\lambda/d \ll 1$ and $\nu_c/\nu_{rf} \gg 1$, where λ is the mean free path of the electrons, d is the electrode spacing, ν_c is the electron collision frequency, and ν_{rf} is the rf oscillation frequency. For these conditions, the electron distribution is spatially isotropic. Energy gained from the applied electric field is proportional to E^2/ν_c where E is the time averaged electric field in the plasma. Electron movement is collisionally dominated, having an acceleration distance equal to the mean free path. In the opposite limit, that is $\lambda/d \gg 1$ and $\nu_c/\nu_{rf} \ll 1$, the energy gained from the electric field is proportional to $Ed\nu_{rf}$. The electron acceleration distance is equal to the electrode spacing and the electron distribution is spatially anisotropic.

For electrons in the body of the plasma, the sheaths represent a positive potential hill which only a small fraction of the electrons are energetic enough to climb. For the conditions $\lambda/l_s \gg 1$, where l_s is the thickness of the sheath, the sheath is collisionless. An electron approaching a sheath from out of the plasma is reflected, returning to the plasma with nearly its incident energy. The electron's encounter with the sheath is analogous to an elastic collision. However, for electrons resulting from ionizations within the sheath or from secondary processes at the electrodes, the sheath appears to be a negative potential hill. These electrons are accelerated out of the sheath, gaining in energy a value nearly equal to the sheath potential. For conditions where secondary electron emission from the electrodes is significant, this source of high energy electrons can contribute a large fraction of the average electron energy to the bulk plasma. These conditions are similar to those in a hollow cathode where the plasma regions have a small electric field. The source of electron energy is electrons emitted from the cathode and accelerated through the sheaths into the plasma.[12]

The spatial differentiation in the sources of electron energy described above is manifested in a spatially and time dependent electron distribution function. In this paper, results from a Monte-Carlo computer simulation are discussed which describe the spatially dependent electron distribution function. Electron trajectories are computed for an rf parallel plate discharge in a molecular gas while oscillating the applied electric field. Many rf cylces are computed while periodically updating the boundary conditions in order to obtain as self-consistent a solution as possible. A time averaged, but spatially dependent electron distribution function is solved for by integrating the electron trajectories in time over many rf cycles. In Sec. II, the model is described. In Secs. III and IV, results from the simulation for the electron distribution function and sheath potential are discussed. Section V contains concluding remarks.

II. DESCRIPTION OF THE MODEL

Initial conditions are assumed for the value of the dc sheath potential and electron temperature. A sample group of electrons, typically 300–500, is randomly seeded between the electrode plates with a Maxwellian distribution. The applied electric field is oscillated at rf frequencies providing a time and spatially dependent electric field, and electron trajectories are calculated using the Monte-Carlo method.[13] A sufficient number of rf cycles are computed to insure that the final results are not sensitive to the choice of initial conditions. When an electron is lost from the plasma as a result of being collected by an electrode or attached to the gas, it is replaced at the site of the most recent ionization, or in the case of secondary electron emission, at the surface of an electrode with an inward directed velocity. The number of electrons which are collected by the electrodes is summed. If after several rf cycles (typically 4 or 5) the flux of electrons to the electrodes differs from the total ionization rate, the dc value of the sheath potential is adjusted appropriately and the process is repeated. During the last set of rf cycles, the spatial location and velocity of each electron is periodically recorded and summed. This final summation yields the time averaged, spatially dependent electron distribution function. The summation involves about 5000 separate recordings of the time varying velocity and position of the electrons. This yields a statistical scatter corresponding to a much larger sample size than the 300–500 electrons typically used in the calculation. In many steady-state calculations using the Monte-Carlo method, the time step chosen for each particle is equal to its collision time for that step. That algorithm could not be used here because of the time dependence of the electric field. All electron trajectories were integrated simultaneously in time using a first order Euler routine.

Since a prohibitively large number of electrons was found to be required to explicitly solve Poisson's equation in the sheath regions, the electric field in the sheath was assumed to be a linear function of distance from the electrode.

$$E(x,t) = \frac{2V_s}{l_s^2}(l_s - x) + E_p(t), \tag{1}$$

where x is the distance from the electrode, l_s is the sheath thickness, and E_p is the electric field in the plasma. V_s is the potential drop across the sheath.

$$V_s(t) = V_{dc} \pm V_{rf}(t)/2, \tag{2}$$

where opposing electrodes take different signs for $V_{rf}(t)$ and $V_{rf}(t) \simeq V_{PP} \sin(2\pi\nu_{rf}t)/2$.

The rf sheath thickness was also solved for in the calculation. On a time averaged basis (ignoring attachment and recombination) the rate at which ions and electrons are lost from the plasma must equal the total ionization rate. During the first half of an rf cycle, the sheath extends into the plasma sweeping ions into the high field region.[14] In the high field region, the electric field does not oscillate in sign and the ions are monotonically accelerated towards the electrodes. During the second half of the rf cycle when the sheath is in retreat, the captured ions are rapidly replaced by diffusion and electron impact ionization of the neutral gas. If the rate at which the ions are collected by the oscillating sheaths is smaller than the total ionization rate, the sheath thickness is increased. If too many ions are collected, the sheath thickness is decreased. Trajectories for the ions were not computed. The flux of ions into the sheath regions was approximat-

Downloaded 27 Mar 2003 to 128.174.115.149. Redistribution subject to AIP license or copyright, see http://ojps.aip.org/japo/japcr.jsp

ed by $n_i(v_t/4 + v_s)$, where n_I is the average ion density, v_t is the average thermal ion velocity, and v_s is the velocity at which the edge of the sheath extends into the plasma. Typically, the rf sheath was found to be a few millimeters thick.

Explicit spatial dependence was included only for the dimension perpendicular to the electrodes surfaces, the x axis. The characteristic dimension parallel to the electrodes, the y axis, was assumed to be large compared to the electron mean free path (a good assumption for our conditions) and therefore effectively infinite. Both the x and y component of the electron velocity were computed. Energy is coupled into the x component through the electric field. Energy is coupled into the y component through collisions, which were assumed to be isotropic.

The specific characteristics calculated for the electron distribution will be a function of the particular gas in the discharge. The purpose of this paper, though, is not to study a particular gas but rather to study the generic molecular gas rf discharge in the capacitively coupled geometry. The conclusions discussed below are insensitive to changes in the particular gas used provided that the electron density is always much larger than the negative ion density, although the specifics do of course change. Results for three different gases will be discussed: CF_4,CO, and N_2. Carbon tetrafluoride was chosen because it is widely used in plasma processing. Carbon monoxide and nitrogen were chosen because their electron impact cross sections are well known and they are mildly attaching and nonattaching gases, respectively. Cross sections for CO were taken from Ref. 15, for CF_4 from Refs. 16–19, and for N_2 from Refs. 15, 20, and 21.

Among the conditions for which this analysis is valid is that the random electron current (i_r) must be much greater than the displacement current (i_d) that is required to charge the series capacitance (C) to the (peak to peak) rf voltage (V_{PP}). To first order, the displacement current and the voltage to which the series capacitance is charged (V_C), obey

$$\left\langle \frac{dV_C}{dt} \right\rangle \simeq 2\nu_{rf} V_{PP} \simeq i_d \left(\frac{A}{C} \right), \tag{3}$$

$$i_d \ll i_r = \left(\frac{8kT_e}{\pi m_e} \right)^{1/2} \frac{n_e e}{2}, \tag{4}$$

where A is the electrode area, T_e is the average electron temperature, m_e is the electron mass, and n_e is the electron density. Equations (3) and (4) set a lower limit on the electron density for which this analysis can be used.

$$\begin{aligned} n_e &\gg \left(\frac{i_d}{e} \right) 2 \left(\frac{\pi m_e}{8kT_e} \right)^{1/2} \\ &\simeq \frac{4\nu_{rf} V_{PP}}{e} \left(\frac{C}{A} \right) \left(\frac{\pi m_e}{8kT_e} \right)^{1/2}. \end{aligned} \tag{5}$$

For the typical values $V_{PP} = 600$ V, $\nu_{rf} = 13.56$ MHz, $C/A = 1$ pF/cm^2, $T_e = 5$ eV, the limit on electron density is $n_e \gg 10^9/\text{cm}^3$.

The electric field outside the sheath regions was assumed to be time varying but spatially uniform. This criteria sets an upper limit on the magnitude of the oscillating electric field, since large values for the field result in unphysically large time averaged variations in the electron density in the plasma. This situation can be avoided for electric fields within the plasma with peak values of about 10 V/cm for nominal operating conditions ($P = 30$ mTorr, $\lambda \simeq 1$ cm). The remainder of the applied voltage is dropped across the sheaths.

III. ELECTRON PROPERTIES AS A FUNCTION OF POSITIONS

Typical computed results for the average electron energy and relative electron density as a function of position between electrodes for a discharge in CF_4 are shown in Fig. 1. The peak to peak applied voltage is 600 V, $\nu_{rf} = 13.56$ MHz, the electrode spacing is 3 cm, and the gas pressure is 50 mTorr. Two cases are plotted: $\gamma \gg 1$ and $\gamma \ll 1$, where γ is the secondary electron emission coefficient for electrons by ion impact on the electrode surfaces.[22] In the bulk plasma, the electron density and average electron energy are essentially constant. For large γ, the electron density

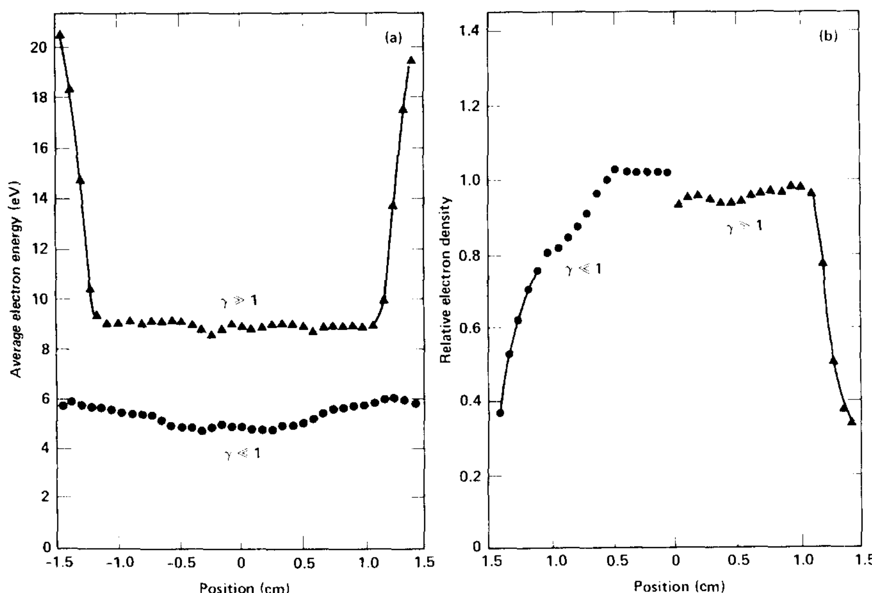

FIG. 1. Computed results for the average electron energy and relative electron density for a discharge in CF_4. The electrode spacing is 3 cm, the gas pressure is 50 mTorr (at 500 K), and the rf frequency is 13.56 MHz. The two cases shown are for $\gamma \gg 1$ and $\gamma \ll 1$, where γ is the secondary electron emission coefficient. The results for electron density have been averaged over the midplane of symmetry at $x = 0$.

Downloaded 27 Mar 2003 to 128.174.115.149. Redistribution subject to AIP license or copyright, see http://ojps.aip.org/japo/japcr.jsp

remains nearly constant until very near the electrodes while the average electron energy increases near the electrodes. For small γ, the average electron energy remains nearly constant near the electrodes. The electron density, though, decreases rapidly near the electrodes, a consequence of there being thicker sheaths than the small γ case and there being no local (i.e., *e*-beam) source of ionization. The significant change in electron density between the two cases is confirmed by recent experimental measurements.[23]

For the conditions where secondary electron emission from the electrodes is large, the results discussed above indicate that the electron distribution function is spatially bimodal. That is, the distribution function has two distinct components with different spatial dependence. In the bulk plasma, the electron distribution is dominated by the thermal component, having an electron temperature nominally in equilibrium with the time averaged electric field. As one approaches the electrodes, the bulk electrons are slowed by the opposing electric field in the sheath, and the bulk electron temperature decreases, as does the bulk electron density. Thermal electrons resulting from ionizations in the sheath, or emitted from the electrodes comprise the second component. These electrons are accelerated from the sheath region into the plasma, creating an *e*-beam component to the electron distribution. As the emitted electrons experience collisions, the average energy of the *e*-beam component decreases with increasing distance from the electrodes. The slowed *e*-beam component eventually joins the bulk distribution, contributing a significant fraction of the bulk electron energy, and thereby accounting for any nonequilibrium conditions that may exist between the bulk electrons and bulk electric field.

Experimental measurements which are typical of the bimodal behavior described above are shown in Fig. 2, where electric probe measurements of the electron flux distribution in CF_4 are plotted as a function of position in a parallel plate rf discharge.[23] Adjacent to the electrode, the distribution is dominated by an *e*-beam component with an averge energy of about 40 eV. At positions further from the electrodes, the *e*-beam component degrades until the lower energy thermal component of the distribution dominates.

Computed flux distributions for a discharge in CO which display bimodal behavior similar to the experimental measurements are plotted in Fig. 3 for conditions where $\gamma \gg 1$. Adjacent to the electrode, the distribution has a relatively small thermal component, and is dominated by the *e*-beam component. Approximately 0.3 cm further from the electrode, the *e*-beam component has both degraded in magnitude relative to the increasingly dominant thermal group, and has also broadened. The majority of the broadening of the *e*-beam component is due to the oscillating electric field in the plasma which alternately accelerates and opposes the *e*-beam component. In addition, the *e*-beam component is broadened on the low energy side by low threshold inelastic collisions which slow the electrons, and on the high side by electrons accelerating through the remainder of the sheath. Finally, at the midpoint between the electrodes, the distribution is essentially thermal, with vestigal evidence of the *e*-beam component near 20 eV.[24]

Computed electron distributions for discharges in CO($\gamma \gg 1$) as a function of position in the discharge are plotted in Fig. 4. In Fig. 4(a), distribution contours are plotted for electron energy less than 11 eV. The low energy distribution function is relatively uniform as a function of position in the middle part of the plasma, which is illustrated by the parallel contour lines. In the sheath regions close to the electrodes, the average energy decreases. This is illustrated by the contours compressing together as one approaches the electrodes. The opposite behavior can be seen in Fig. 4(b), where the distribution contours are plotted for electron energy less than 80 eV. The contours, initially wide apart near the electrodes compress as one traverses the plasma toward the center line, reflecting a decrease in the average energy of the high energy component resulting from inelastic collisions.

The degree of spatial dependence in the electron distribution function changes with the specific gas used in the discharge. For otherwise constant conditions (e.g., constant applied voltage, plate separation, and gas pressure), nitrogen

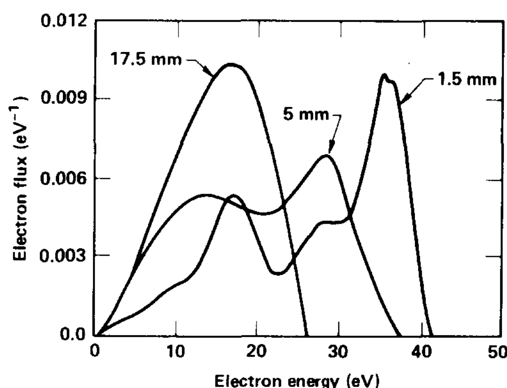

FIG. 2. Electric probe measurements for the electron flux distribution for a CF_4 discharge in an rf parallel plate plasma etching reactor. The peak to peak rf voltage was 590 V, electrode separation was 3.5 cm, and the gas pressure was 22 mTorr. The measurements were made (a) 1.5 mm, (b) 5 mm, and (c) 17.5 mm from the electrodes.

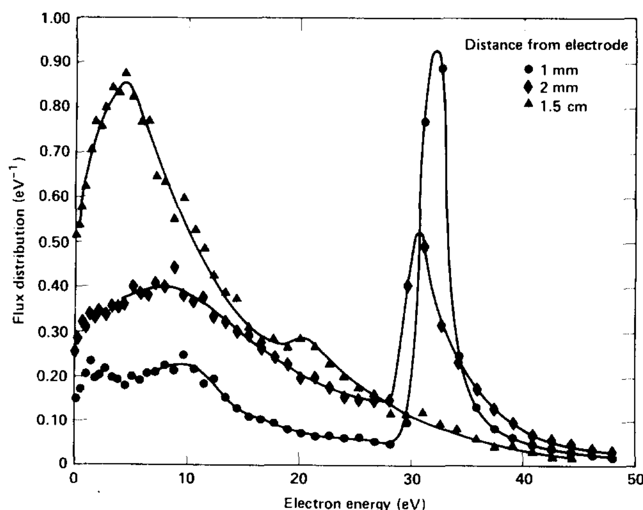

FIG. 3. Computed electron flux distributions for an rf discharge in CO for $\gamma \gg 1$. The gas pressure is 20 mTorr and electrode separation 3 cm. The distributions have been separately normalized at each spatial position.

Downloaded 27 Mar 2003 to 128.174.115.149. Redistribution subject to AIP license or copyright, see http://ojps.aip.org/japo/japcr.jsp

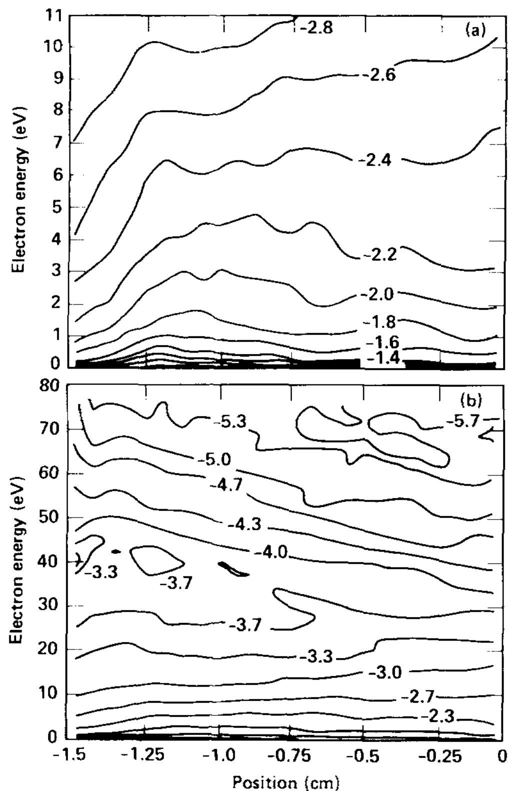

FIG. 4. Computed electron distributions as function of position and energy for a discharge in CO and the conditions of Fig. 3. The two plots are for electron energy (a) 0–11 eV and (b) 0–80 eV. These results were averaged across the midplane of symmetry of the discharge (x = 0). The contour labels are the values of $\log[f(\epsilon)]$, where $f(\epsilon)$ is the electron distribution function ($eV^{-3/2}$) for electron energy ϵ. The distributions have been normalized to unity at each spatial location.

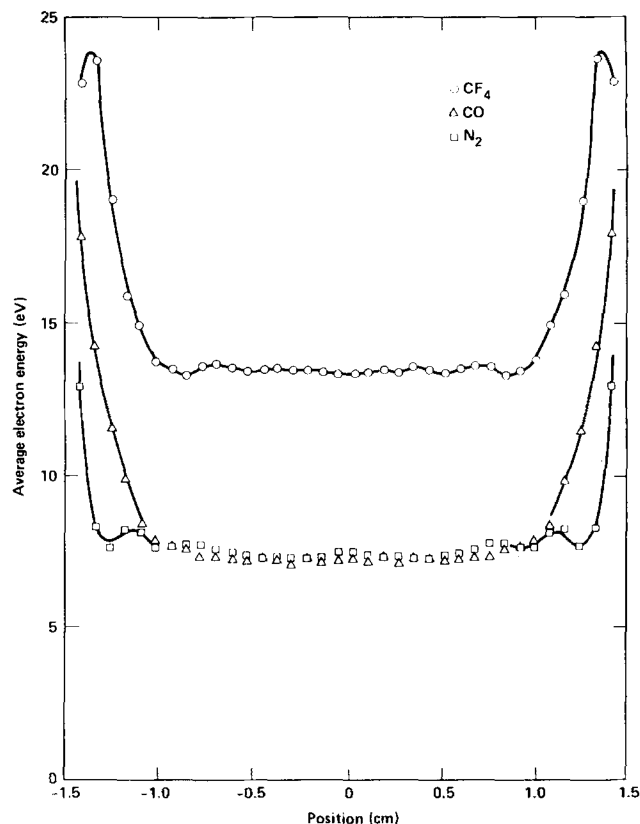

FIG. 5. Computed average electron energy for discharges in N_2, CO, and CF_4 as a function of position between the electrodes. The gas pressure is 20 mTorr and the electrode spacing is 3 cm. The dc sheath potential for the gases are 175, 160, and 150 V, respectively.

and carbon monoxide displayed similar spatial behavior, while carbon tetrafluoride displayed the greatest spatial differentiation. In Fig. 5, computed average electron energy is plotted as a function of position between the electrodes for the three gases for the same pressure and applied voltage Very high average energy is obtained in CF_4 both in the plasma and near the sheaths, as was found experimentally.[23] For discharges in N_2 and CO, the average electron energy outside of the sheath regions is nearly the same. In the *e*-beam dominated sheath regions, CO has a higher average electron energy inspite of the fact that the dc sheath potential of the N_2 discharge is larger. In the absence of secondary electron emission, though, the average electron energy in the bulk plasma for CO and N_2 differ significantly. In N_2, the average bulk electron energy is 5 eV, while in CO the value is 3.5 eV. The contribution to the average electron energy by the *e*-beam component is seen to be larger in CO than in N_2. The amount of this contribution can amount to about 35%, as illustrated in fig. 1.

The spatial differentiation in the electron distribution is reflected in the relative frequency at which inelastic collisions occur as a function of position in the plasma. The time averaged excitation rate is given by

$$r(x) = \frac{1}{T}\int_0^T \int_0^\infty n_e(x,\epsilon,t) f(x,\epsilon,t)\sigma(\epsilon)\left(\frac{2\epsilon}{m_e}\right)^{1/2} d\epsilon\, dt, \quad (6)$$

where $n_e(x, \epsilon, t)$ is the electron density, $f(x, \epsilon, t)$ is the electron distribution function, and $\sigma(\epsilon)$ is the cross section for electron energy ϵ, at spatial location x, and at time t. For electronic excitation and ionization, $\sigma(\epsilon)$ increases with increasing electron energy for the values of interest. Therefore, one would expect relatively large excitation rates very near the electrodes. We have already seen, though, that the electron density decreases in these same regions. The net affect is that the excitation rate is small near the electrodes, with larger rates being found at intermediate locations in the plasma.

Time averaged excitation rates calculated as a function of position are plotted in Fig. 6 for a discharge in $N_2(\gamma \gg 1)$. The ionization rate, with a high threshold energy, has a maximum value relatively close to the sheaths where the high energy *e*-beam component dominates. The ionization rate is relatively constant in the middle of the discharge.[25] In the absence of a large *e*-beam component, the ionization rate maximizes further from the electrode (see Fig. 7). The electronic excitation rate has a maximum value at a location further from the electrodes, a result of a lower threshold energy, and optimization at lower electron energy (see Fig. 6). The cross section for vibrational excitation is resonant, and nonzero only for electron energy less than about 8 eV. The excitation rate is therefore nearly idependent of the *e*-beam component, and a function only of the bulk plasma properties. The rate maximizes near the center of the dis-

Downloaded 27 Mar 2003 to 128.174.115.149. Redistribution subject to AIP license or copyright, see http://ojps.aip.org/japo/japcr.jsp

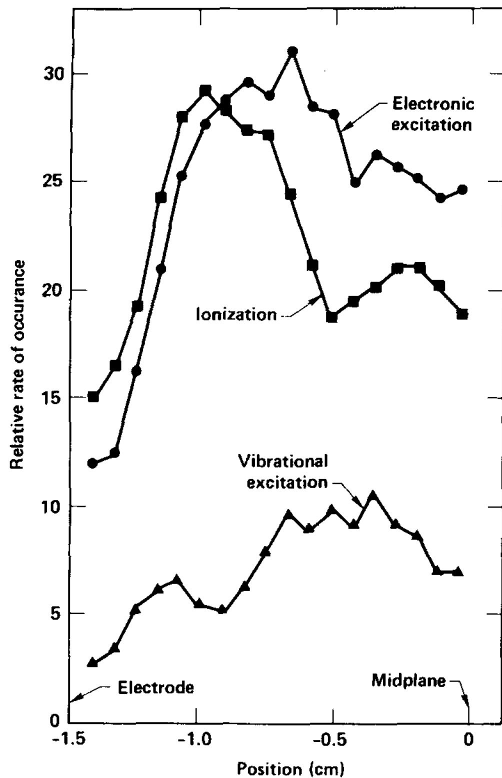

FIG. 6. Calculated electron collision rates for ionization, electronic excitation, and vibrational excitation as a function of position for a discharge in nitrogen (pressure = 75 mTorr). The rates have been averaged across the midplane of symmetry of the discharge ($x = 0$).

charge.

IV. THE dc SHEATH POTENTIAL

The average mean free path of electrons λ for the conditions of Fig. 3 is approximately 0.6 cm, yielding a value for λ/d of 0.2. The value of the dc sheath potential is a function of the ratio λ/d. Consider the conditions where $\lambda/d \gg 1$. For this discharge, the average electron samples the sheath region near the electrodes at least once after every collision. Concurrently, electrons emitted from one electrode will, with a high probability, traverse the discharge and impinge on the opposite sheath. As a result, the rate at which electrons are collected by the electrodes in large. The response of the system is to increase the dc component of the sheath potential in order to reduce the electron flux to the electrodes while simultaneously increasing the ion flux.

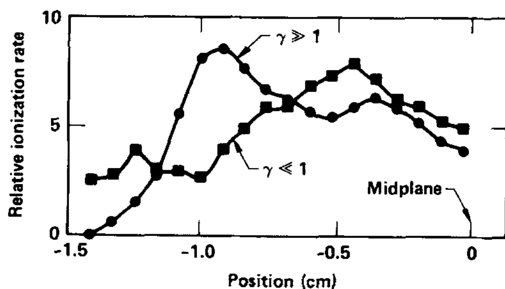

FIG. 7. Electron impact ionization rate for a discharge in nitrogen (pressure = 20 mTorr) in the presence ($\gamma \gg 1$) and in the absence ($\gamma \ll 1$) of secondary electron emission.

Increasing the dc sheath potential in order to reduce the electron flux to the electrodes appears at first glance to be an unstable solution to the problem. A larger dc sheath potential intended to slow the electron flux to one electrode provides a higher energy electron flux to the opposite electrode from secondary electrons falling through the higher (negative) potential. The saving factor is that collisions do occur in the plasma which slow down the emitted electrons. Electrons emitted from an electrode which traverse the plasma and are reflected by the opposite sheath will, in the worst case, continue to oscillate between sheaths until inelastic, or randomizing collisions occur. In addition, unless the oscillation period of the emitted electron is in phase with the applied electric field, the electron will, on the average, be opposed by that electric field, eventually slowing down and joining the bulk distribution.

For conditions where $\lambda/d \ll 1$, the average electron samples the sheath region only after many collisions and electrons emitted from an electrode are quickly thermalized in the plasma. The dc sheath potential responds only to the bulk plasma properties and has a relatively constant value.

Computed dc sheath potentials as a function of electrode spacing (for constant gas pressure) and gas pressure (for constant electrode spacing) for discharges in CO are plotted in Fig. 8. The independent variable in Fig. 8 is $d*p$, the product of the electrode spacing times the gas pressure. The electron mean free path remains fairly constant as the electrode spacing is changed, and is inversely proportional to the gas pressure. Therefore, positive displacement along the horizontal axis decreases in the ratio λ/d. For large electrode spacing ($\lambda/d \ll 1$) the dc sheath potential is nearly constant. When the electrode spacing gets sufficiently small, though, the dc sheath potential increases in response to the higher rate at which bulk electrons are collected by the electrodes and the high energy electron flux generated by the approaching opposite sheath. Similar behavior is observed when the electrode spacing is held constant and the gas pressure is reduced, thereby increasing λ/d. The response of the dc sheath potential, though, is not as dramatic when the gas pressure is reduced as when the electrode spacing is reduced.

Recent experimental measurements have been made of the dc negative bias in a parallel plate rf reactor similar to our geometry.[10] For a variety of gases, the dc bias was found to increase (negative) as the gas pressure was reduced and the mean free path of the electrons increased. This observation is consistent with the discussion above.

Computed electron distribution functions for electrode separations of 2, 2.5, and 4 cm are plotted in Fig. 9. As the electrode separation decreases, the average electron samples the sheath regions more frequently and the average electron acceleration distance decreases. The result is that the average energy of the bulk electrons decreases with progressively smaller electrode separation. This effect is illustrated in Fig. 9 by the more closely spaced parallel contours for the electron distribution function in the middle of the plasma. The dc sheath potential, though, increases as the electrode spacing decreases, thereby providing a more energetic e-beam component. This effect is illustrated in Fig. 9 by the progres-

Downloaded 27 Mar 2003 to 128.174.115.149. Redistribution subject to AIP license or copyright, see http://ojps.aip.org/japo/japcr.jsp

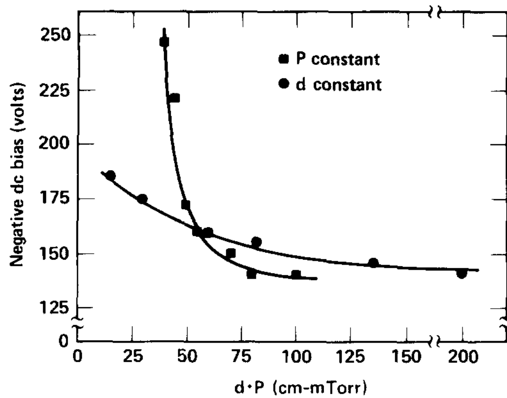

FIG. 8. Computed dc sheath potential for discharges in CO as a function of $d*p$, the product of the electrode spacing times the gas pressure. The cases are for (■) constant pressure and (●) constant electrode spacing.

sively steeper contours near the electrodes. The combined effect is that the electron distribution function is nearly uniform as a function of position for large electrode separation and becomes more spatially differentiated as that distance decreases.

V. CONCLUDING REMARKS

Electron properties in a parallel plate, capacitively coupled rf discharge have been examined with results from a Monte-Carlo simulation. The electron distribution function has a low energy thermal group, and a high energy *e*-beam component, a result of secondary electron emission from the electrodes. The high energy component dominates the electron distribution near the electrodes where the sheath potential excludes the lower energy bulk plasma component. Electron impact excitation rates have spatial dependence as well. Processes with a high threshold energy have large excitation rates near the electrodes, while processes with lower threshold energy have rates which maximize deeper into the plasma. The dc sheath potential is a function of the ratio λ/d. Large (negative) values for the sheath potential are obtained when λ/d is large.

ACKNOWLEDGMENT

The author would like to thank Dr. L. C. Pitchford of Sandia National Laboratories for suggesting a number of topics investigated in this study.

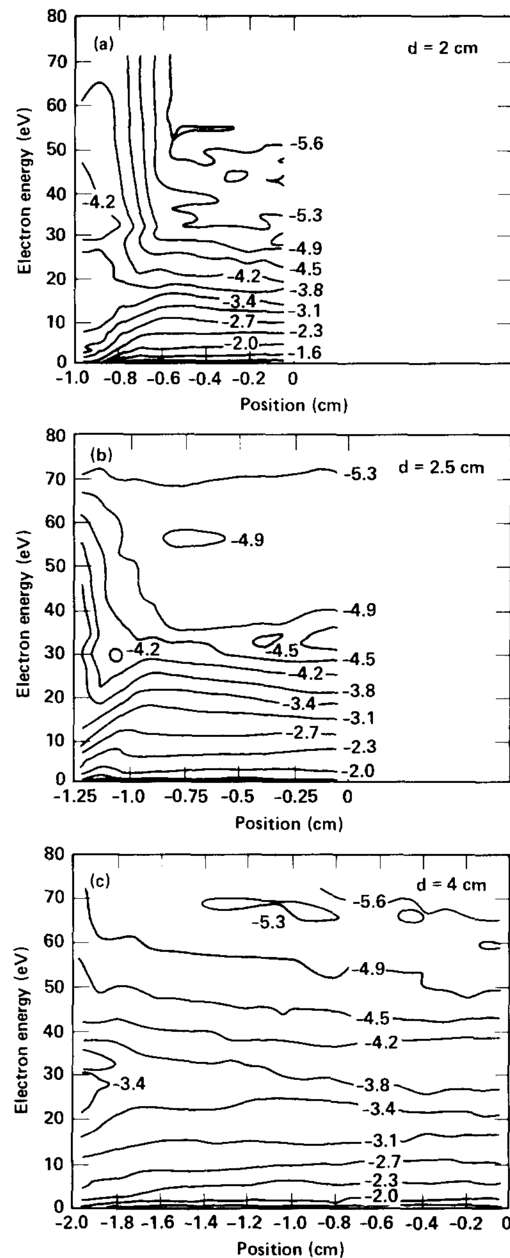

FIG. 9. Computed electron distributions for discharges in CO ($P = 30$ mTorr) as a function of position in the plasma. The results have been averaged over the midplane of symmetry ($x = 0$), and the notation is the same as in Fig. 4. The cases are for electrode separations of (a) cm, (b) 2.5 cm, and (c) 4 cm.

[1]D. L. Flamm and V. M. Donnelly, Plasma Chem. Plasma Proc. **1**, 317 (1981).
[2]T. P. Chow and A. J. Steckl, J. Appl. Phys. **53**, 5531 (1982).
[3]J. W. Coburn and E. Kay, IBM J. Res. Dev. **23**, 33 (1979).
[4]B. Chapman, *Glow Discharge Processes: Sputtering and Plasma Etching* (Wiley, New York, 1980), pp. 297–349.
[5]C. S. Korman, J. Vac. Sci. Technol. **20**, 476 (1982).
[6]R. A. Gottscho, G. Smolinsky, and R. H. Burton, J. Appl. Phys. **53**, 5908 (1982).
[7]C. J. Mogab, A. C. Adams, and D. L. Flamm, J. Appl. Phys. **49**, 3796 (1978).
[8]J. L. Vossen, J. Electrochem. Soc. **126**, 319 (1979).
[9]J. W. Coburn and E. Kay, J. Appl. Phys. **43**, 4965 (1972).
[10]R. A. Morgan, Vacuum **32**, 297 (1982).
[11]M. Mitchner and C. H. Kruger, *Partially Ionized Gases* (Wiley, New York, 1973), pp. 129–134.
[12]B. E. Warner and K. B. Person, J. Appl. Phys. **50**, 5964 (1979).
[13]J. Lucas, Int. J. Electron. **32**, 393 (1972).
[14]See, for example, the Child–Langmuir theory for sheaths, and time dependent treatments for expanding sheaths. J. D. Cobine, *Gaseous Conductors: Theory and Engineering Applications* (Dover, New York, 1958); K. F. Sander, J. Plasma Phys. **3**, 353 (1969); R. H. Varey and K. F. Sander, J. Phys. D **2**, 40 (1969); A. G. Jack, K. F. Sander, and R. H. Varey, J. Plasma Phys. **5**, 211 (1971).
[15]L. J. Kieffer, "*A Compilation of Electron Collision Cross-Section Data for Modelling Gas Discharge Lasers*," Joint Institute for Laboratory Astrophysics COM-74-11661, Boulder, CO (1973), pp. 61–91.
[16]M. S. Naidu and A. N. Prasad, J. Phys. D **5**, 983 (1972).
[17]P. W. Harland and J. L. Franklin, J. Chem. Phys. **61**, 1621 (1974).
[18]Y. Itikawa, J. Phys. Soc. Jpn. **36**, 1121 (1974).
[19]H. F. Winters and M. Inokuti, Phys. Rev. A **25**, 1420 (1982).
[20]L. C. Pitchford and A. V. Phelps, Phys. Rev. A **25**, 540 (1982).
[21]K. Tachibana and A. V. Phelps, J. Chem. Phys. **71**, 3544 (1979).

Downloaded 27 Mar 2003 to 128.174.115.149. Redistribution subject to AIP license or copyright, see http://ojps.aip.org/japo/japcr.jsp

[22]The secondary electron emission coefficient is rarely larger than a few tenths. A large value for γ was chosen here in order to contrast the two limiting cases: where secondary emission is negligible and where secondary emission dominates.
[23]M. J. Kushner, J. Appl. Phys. **53**, 2939 (1982).
[24]Similar bimodal electron distribution functions have been computed for the cathode region of a glow discharge. J. P. Boeuf and E. Marode, J. Phys. D **15**, 2169 (1982).
[25]This observation is consistent with recent spectroscopic measurements made of ion densities in a CCl_4 rf plasma. V. M. Donnelly, D. L. Flamm, and G. Collins, J. Vac. Sci. Technol. **21**, 817 (1982).

Downloaded 27 Mar 2003 to 128.174.115.149. Redistribution subject to AIP license or copyright, see http://ojps.aip.org/japo/japcr.jsp